


Observation of a $J/\psi\Lambda$ Resonance Consistent with a Strange Pentaquark Candidate in $B^- \rightarrow J/\psi\Lambda\bar{p}$ Decays

R. Aaij *et al.**
(LHCb Collaboration)

 (Received 24 October 2022; accepted 12 January 2023; published 17 July 2023)

An amplitude analysis of $B^- \rightarrow J/\psi\Lambda\bar{p}$ decays is performed using 4400 signal candidates selected on a data sample of pp collisions recorded at center-of-mass energies of 7, 8, and 13 TeV with the LHCb detector, corresponding to an integrated luminosity of 9 fb^{-1} . A narrow resonance in the $J/\psi\Lambda$ system, consistent with a pentaquark candidate with strangeness, is observed with high significance. The mass and the width of this new state are measured to be $4338.2 \pm 0.7 \pm 0.4 \text{ MeV}$ and $7.0 \pm 1.2 \pm 1.3 \text{ MeV}$, where the first uncertainty is statistical and the second systematic. The spin is determined to be $1/2$ and negative parity is preferred. Because of the small Q -value of the reaction, the most precise single measurement of the B^- mass to date, $5279.44 \pm 0.05 \pm 0.07 \text{ MeV}$, is obtained.

DOI: [10.1103/PhysRevLett.131.031901](https://doi.org/10.1103/PhysRevLett.131.031901)

The discovery of pentaquark candidates in the $J/\psi p$ system at LHCb [1,2] opened a new field of investigation in baryon spectroscopy. Such resonant structures with valence quark content (the exotic hadron naming scheme defined in Ref. [3] is used throughout this Letter) $P_{\psi}^{N+} = c\bar{c}uud$ have been observed only in the $\Lambda_b^0 \rightarrow J/\psi p K^-$ decay to date. Recently, evidence for a new candidate was found in the $B_s^0 \rightarrow J/\psi p \bar{p}$ decay [4,5], and evidence for a $P_{\psi_s}^{\Lambda 0} = c\bar{c}uds$ pentaquark candidate with strangeness was found in the $J/\psi\Lambda$ system in the $\Xi_b^- \rightarrow J/\psi\Lambda K^-$ decay [6] (charge conjugation is implied throughout this Letter).

Pentaquarks are predicted within the quark model to have a minimal quark content of three quarks plus a quark-antiquark pair. Experimentally, the pentaquark candidates are found close to threshold for the production of ordinary baryon-meson states, i.e., $\Sigma_c^+ \bar{D}^0$ and $\Sigma_c^+ \bar{D}^{*0}$ for the observed P_{ψ}^{N+} states [1,2] and $\Xi_c^0 \bar{D}^{*0}$ for the $P_{\psi_s}^{\Lambda 0}$ state [6]. Various interpretations of these states have been proposed, including tightly bound pentaquark states [7,8], loosely bound baryon-meson molecular states (Refs. [9,10] and references therein), and rescattering effects [11]. Hidden-charm pentaquarks with strangeness were predicted in Refs. [12,13] as hadronic molecules, and in Ref. [14] as compact states. However, their nature is still largely unknown and further investigation is needed [15].

The $B^- \rightarrow J/\psi\Lambda\bar{p}$ decay offers the unique opportunity to simultaneously search for \bar{P}_{ψ}^{N-} and $P_{\psi_s}^{\Lambda 0}$ pentaquark candidates in the $J/\psi\bar{p}$ and $J/\psi\Lambda$ systems, respectively. In particular, the phase space available in the decay allows searches for pentaquark candidates located close to different baryon-meson thresholds, such as $\Lambda_c^+ D^0$ for P_{ψ}^{N+} , and $\Lambda_c^+ D_s^-, \Xi_c^+ D^-$ for $P_{\psi_s}^{\Lambda 0}$ candidates. Neither the $P_{\psi_s}^{\Lambda}(4459)^0$ state found in the $\Xi_b^- \rightarrow J/\psi\Lambda K^-$ decay [6] nor the $P_{\psi}^N(4337)^+$ state found in the $B_s^0 \rightarrow J/\psi p \bar{p}$ decays [5] is accessible with the present analysis since they are outside of the available phase space.

The small Q -value of the decay, approximately (natural units with $\hbar = c = 1$ are used throughout this Letter) 128 MeV, provides excellent mass resolution, allowing searches for narrow resonant structures. In addition, efficient reconstruction of low momentum tracks can improve sensitivity to resonance structures near threshold. This decay was previously studied by the CMS Collaboration using a sample of 450 ± 20 signal candidates, and the invariant-mass distributions of the $J/\psi\Lambda$, $J/\psi\bar{p}$, $\Lambda\bar{p}$ systems were found to be inconsistent with the pure phase-space hypothesis [16]. In this Letter, an amplitude analysis of the $B^- \rightarrow J/\psi\Lambda\bar{p}$ decay is performed using signal candidates selected on a data sample of pp collisions at center-of-mass energies of 7 and 8 TeV (Run 1), and 13 TeV (Run 2) recorded between 2011 and 2018 by the LHCb detector, corresponding to an integrated luminosity of 9 fb^{-1} . In the following, the first observation of a $P_{\psi_s}^{\Lambda 0}$ pentaquark candidate with strangeness in the $J/\psi\Lambda$ system is reported, which is different from the $P_{\psi_s}^{\Lambda}(4459)^0$ state found in the $\Xi_b^- \rightarrow J/\psi\Lambda K^-$ decay [6].

The LHCb detector is a single-arm forward spectrometer covering the pseudorapidity range $2 < \eta < 5$ described in detail in Refs. [17–20]. The online event selection is

*Full author list given at the end of the article.

performed by a trigger [21] comprising a hardware stage based on information from the muon system which selects $J/\psi \rightarrow \mu^+\mu^-$ decays, followed by a software stage that applies a full event reconstruction. The software trigger relies on identifying J/ψ decays into muon pairs consistent with originating from a B -meson decay vertex detached from the primary pp collision point.

Samples of simulated events are used to study the properties of the signal mode decay $B^- \rightarrow J/\psi\Lambda(\rightarrow p\pi^-)\bar{p}$ and the control-mode decay $B^- \rightarrow J/\psi K^*(892)^- [\rightarrow K_S^0(\rightarrow \pi^+\pi^-)\pi^-]$. The latter are used to calibrate the distributions of simulated B^- decays with the data.

The pp collisions are generated using PYTHIA [22] with a specific LHCb configuration [23]. Decays of hadronic particles and interactions with the detector material are described by EvtGen [24], using PHOTOS [25], and by the GEANT4 toolkit [26–28], respectively. The signal and the control-mode decays are generated from a uniform phase-space distribution.

Signal B^- candidates are formed from combinations of J/ψ , Λ , and \bar{p} candidates originating from a common decay vertex. The J/ψ candidates are formed from pairs of oppositely charged tracks identified as muons and originating from a decay vertex significantly displaced from the associated pp primary vertex (PV). The associated PV for a given particle is the PV with the smallest impact parameter χ_{IP}^2 defined as the difference in the vertex-fit χ^2 of a given PV reconstructed with and without the particle under consideration. The $\Lambda \rightarrow p\pi^-$ candidates are formed from pairs of oppositely charged tracks and selected in two different categories according to the Λ decay position: (i) the “long” category for early decays that allow the proton and pion candidates to be reconstructed in the vertex detector; (ii) the “downstream” category for Λ baryons that decay outside the vertex detector and are reconstructed in the tracking stations only. The long candidates have better mass, momentum, and vertex resolution than the downstream candidates. The \bar{p} candidate is a charged track identified as an antiproton.

A kinematic fit [29] to the B^- candidate is performed with the dimuon and the $p\pi^-$ masses constrained to the known J/ψ and Λ masses, respectively [30]. Simulated events are weighted such that the distributions of transverse momentum (p_T) and number of tracks per event for B^- candidates match the $B^- \rightarrow J/\psi K^*(892)^-$ control-mode distributions in the data. In simulation, the particle identification (PID) variables for each charged track are resampled as a function of their p , p_T , and the number of tracks in the event using $\Lambda_c^+ \rightarrow pK^-\pi^+$ and $D^{*+} \rightarrow D^0(\rightarrow K^-\pi^+)\pi^+$ calibration samples from the data [31].

The final stage of the selection uses multivariate techniques trained with simulation and data. Separate boosted-decision-tree (BDT, [32]) classifiers are employed for the four combinations of two data-taking periods (Run 1 and Run 2) and two signal categories, using long and downstream

reconstructed Λ candidates. Each BDT is trained on simulated signal decays and data sidebands, with the $m(J/\psi\Lambda\bar{p})$ invariant mass in the range [5320, 5360] MeV. The variables used as input to the BDT are the p_T , the decay length significance, the angle between the momentum and the flight direction, and the χ_{IP}^2 variable of the B^- candidate; the χ^2 probability from the kinematic fit of the candidate; the sum of the χ_{IP}^2 of the daughter particles; the angle between the momentum and the flight direction, the χ^2 of the flight distance (only for long category candidates), the χ_{IP}^2 variables of the Λ candidate, and the hadron PID for the \bar{p} candidate from the ring-imaging Cherenkov detectors.

The BDT output selection criterion is chosen as in Ref. [5] by maximizing the figure of merit $S^2/(S+B)^{3/2}$ to obtain both high signal purity and significance, where S and B are the signal and background yield in a region of ± 5.3 MeV around the known B^- mass. To avoid a possible bias due to fluctuations of the signal yield, S is determined from a fit to the $J/\psi\Lambda\bar{p}$ invariant-mass distribution in the data after applying a loose BDT selection, multiplied by the efficiency of the BDT output requirement obtained from simulation. Similarly, B is extracted from a fit to sideband data.

For candidates passing all selection criteria, a maximum-likelihood fit is performed to the $m(J/\psi\Lambda\bar{p})$ distribution shown in Fig. 1, resulting in a signal yield of 4620 ± 70 . For the amplitude analysis, about 4400 signal candidates are retained, with a purity of 93.0% in the signal region of $\pm 2.5\sigma$ around the mass peak, where $\sigma \approx 2.1$ MeV is the mass resolution. The signal distribution is modeled by the sum of a Johnson function [33] and two Crystal Ball [34] functions sharing the same mean and width parameters determined from the fit. The tail parameters and fractions of each signal component are fixed to values obtained from a fit to simulated events. The background contribution is mainly due to random combinations of charged particles in the event and is described by a third-order Chebyshev polynomial.

The Dalitz distribution of the reconstructed B^- candidates in the signal region is shown in Fig. 2, where a

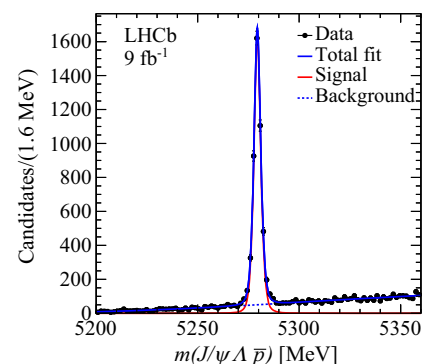


FIG. 1. Invariant-mass distribution of the $J/\psi\Lambda\bar{p}$ candidates. The data are overlaid with the results of the fit.

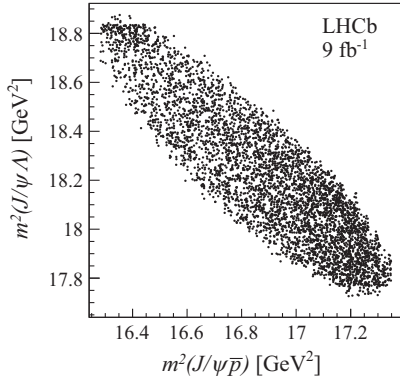


FIG. 2. Dalitz distribution for B^- candidates in the signal region.

horizontal band in the region around 18.8 GeV^2 in the $m^2(J/\psi\Lambda)$ distribution is present. Some structure in the high $m^2(J/\psi\bar{p})$ spectrum is also present. This Letter investigates the nature of these enhancements.

An amplitude analysis of the B^- candidates in the signal region is performed using a phenomenological model based on the interference of two-body resonances in the three decay chains $J/\psi K^{*-}(\rightarrow \Lambda\bar{p})$, $\Lambda\bar{P}_{\psi}^{N-}(\rightarrow J/\psi\bar{p})$, and $\bar{p}P_{\psi s}^{\Lambda 0}(\rightarrow J/\psi\Lambda)$ labeled as the K^{*-} , \bar{P}_{ψ}^{N-} , and $P_{\psi s}^{\Lambda 0}$ chains, respectively. The angular information of the subsequent $J/\psi \rightarrow \mu^+\mu^-$ and $\Lambda \rightarrow p\pi^-$ decays are taken into account in all cases. The decay amplitudes are based on helicity formalism [35] with CP symmetry enforced, and follow the prescriptions in Ref. [36] for the spin alignment of the different decay chains. Details about the decay amplitude definition are given in the Supplemental Material [37].

The decay amplitudes are defined as a function of the six-dimensional phase space of the B^- decay, $(m_{\Lambda\bar{p}}, \vec{\Omega})$ described by the combined invariant mass $m_{\Lambda\bar{p}}$ of the \bar{p} and Λ pairs, and by five angular variables indicated as $\vec{\Omega}$: the cosine of the helicity angle $\cos\theta_{K^*}$ ($\cos\theta_{J/\psi}$) of the Λ (μ^-) in the $\Lambda\bar{p}$ (J/ψ) rest frame, the azimuthal angle ϕ_p (ϕ_{μ^-}) of the p (μ^-) in the rest frame of the Λ (J/ψ), and the cosine of the helicity angle $\cos\theta_{\Lambda}$, of the p in the rest frame of the Λ . The amplitude fit to determine the model parameters $\vec{\omega}$, i.e., the couplings, the masses, the widths, and line shape parameters of different contributions, is performed by minimizing the negative log-likelihood function,

$$-2 \log \mathcal{L}(\vec{\omega}) = -2 \sum_i \log[(1 - \beta) \mathcal{P}_{\text{sig}}(m_{\Lambda\bar{p},i}, \vec{\Omega}_i | \vec{\omega}) + \beta \mathcal{P}_{\text{bkg}}(m_{\Lambda\bar{p},i}, \vec{\Omega}_i)], \quad (1)$$

where \mathcal{P}_{sig} (\mathcal{P}_{bkg}) is the probability density function (PDF) for the signal (background) component of the i th event, and $\beta = 0.07 \pm 0.01$ is the fraction of background candidates in the signal region. The signal PDF is proportional to the squared decay amplitude $|\mathcal{M}(m_{\Lambda\bar{p}}, \vec{\Omega} | \vec{\omega})|^2$ and accounts

for the phase-space element $\Phi(m_{\Lambda\bar{p}})$ and the reconstruction efficiency $\epsilon(m_{\Lambda\bar{p}}, \vec{\Omega})$,

$$\mathcal{P}_{\text{sig}}(m_{\Lambda\bar{p}}, \vec{\Omega} | \vec{\omega}) = \frac{|\mathcal{M}(m_{\Lambda\bar{p}}, \vec{\Omega} | \vec{\omega})|^2 \Phi(m_{\Lambda\bar{p}}) \epsilon(m_{\Lambda\bar{p}}, \vec{\Omega})}{I(\vec{\omega})}. \quad (2)$$

The denominator $I(\vec{\omega})$ normalizes the probability. The background PDF \mathcal{P}_{bkg} is parametrized according to a six-dimensional phase-space function based on Legendre polynomials, whose coefficients are determined from the $m(J/\psi\Lambda\bar{p})$ region $[5200, 5250] \cup [5340, 5350] \text{ MeV}$. Similarly, the reconstruction efficiency is parametrized using Legendre polynomials with coefficients determined using simulated phase-space signal decays.

No well-established resonances are expected to decay into the $J/\psi\Lambda$ and $J/\psi\bar{p}$ final states. However, excited K^- resonances decaying outside of the phase space of the $B^- \rightarrow J/\psi\Lambda\bar{p}$ decay can contribute to the $\Lambda\bar{p}$ channel [16]. A fit including only NR contributions and $K_4^*(2045)^-$, $K_2(2250)^-$, and $K_3(2320)^-$ resonant amplitudes does not reproduce the data distribution. A $\chi^2/\text{n.d.f.}$ of 123.2/46 is obtained, where the χ^2 is calculated as the largest value over the six one-dimensional fit projections and the number of degrees of freedom (n.d.f.) is extracted from pseudoexperiments by fitting the tail of the χ^2_{max} distribution. The simplest and most effective amplitude model used to fit the data, indicated as the nominal model in the following, comprises a narrow $J/\psi\Lambda$ structure with spin parity $J^P = 1/2^-$, whose mass and width are extracted from the amplitude fit, and two nonresonant (NR) contributions, one with $J^P = 1^-$ for the $\Lambda\bar{p}$ system and a second one with $J^P = 1/2^-$ for the $J/\psi\bar{p}$, referred to as NR($\Lambda\bar{p}$) and NR($J/\psi\bar{p}$), respectively. The $J/\psi\Lambda$ resonance is modeled with a relativistic Breit-Wigner function as discussed in the Supplemental Material [37].

The couplings are defined in the LS basis, both for the $B^- \rightarrow XR$ process and for the $R \rightarrow YZ$ process, where X , Y , and Z are the final state particles, and $R = K^{*-}$, \bar{P}_{ψ}^{N-} , and $P_{\psi s}^{\Lambda 0}$ is the decay chain under consideration. Here, L indicates the decay orbital angular momentum, and S is the sum of the spins of the decay products. In the nominal model, $L = 0$ is used for the production and decay of the narrow $J/\psi\Lambda$ resonance, while $L = 0, 1, 2$ and $L = 0, 2$ are used in the NR($\Lambda\bar{p}$) system for the production and decay, respectively, and $L = 0$ and $L = 1$ in the NR($J/\psi\bar{p}$) system. Because of the small Q -value of the decay, higher values of the orbital momentum are suppressed. Fixing the lowest orbital momentum couplings for the NR($J/\psi\bar{p}$) as the normalization choice reduces the number of free parameters to 16: the mass, the width, and the complex coupling of the $P_{\psi s}^{\Lambda 0}$ resonant contribution, four complex couplings for the NR($\Lambda\bar{p}$) contribution, and

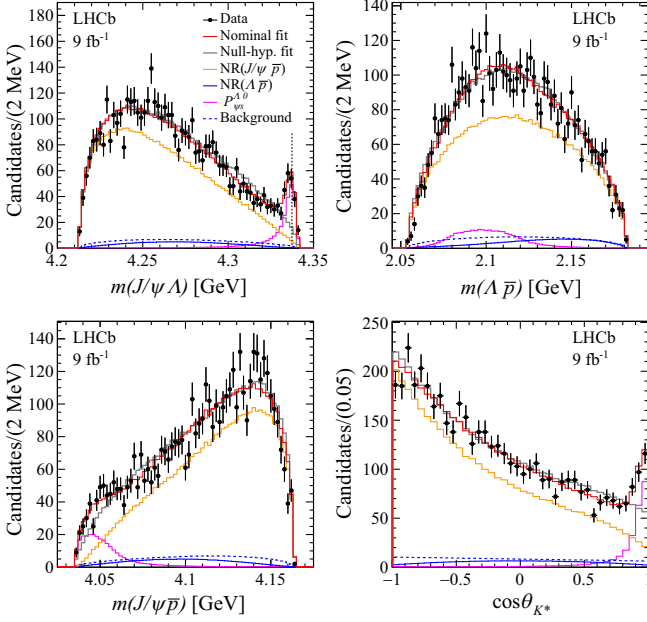


FIG. 3. Distributions of invariant mass and $\cos \theta_{K^*}$. Fit results to the data using the nominal model are superimposed. The null-hypothesis model fit results are also shown in gray. The $\Xi_c^+ D^-$ baryon-meson threshold at 4.337 GeV is indicated with a vertical dashed line in the $m(J/\psi \Lambda)$ invariant-mass distribution.

a complex coupling and two parameters for the second-order polynomial parametrization of the line shape for the NR($J/\psi \bar{p}$) contribution.

A null-hypothesis model is used to test the significance of the $P_{\psi_s}^{\Lambda 0}$ state, which comprises only two NR contributions. The fit results for the nominal and the null-hypothesis model are shown in Fig. 3. The null-hypothesis model does not describe the data, with a corresponding $\chi^2_{\max}/\text{n.d.f.} = 120.8/47$. Using the nominal model, a good fit to the data was obtained with a $\chi^2_{\max}/\text{n.d.f.} = 55.3/51$ and a p -value of 0.51 computed by counting the number of pseudoexperiments above the value of χ^2_{\max} observed in the data.

A new narrow $J/\psi \Lambda$ structure is observed with high significance in the nominal fit to the data. Using Wilks's theorem, a statistical significance exceeding 15σ is estimated from the value of $-2\Delta \log \mathcal{L} = 243$ of the null-hypothesis model with respect to the nominal model. The mass and width of the new pentaquark candidate are measured to be $M_{P_{\psi_s}^{\Lambda}} = 4338.2 \pm 0.7$ MeV and $\Gamma_{P_{\psi_s}^{\Lambda}} = 7.0 \pm 1.2$ MeV, respectively, where the uncertainties are statistical only. This represents the first observation of a strange pentaquark candidate with minimal quark content $c\bar{c}uds$.

Alternative models are considered for systematic studies. To assess the contribution of a \bar{P}_{ψ}^{N-} pentaquark candidate, a relativistic Breit-Wigner function is used for the $m(J/\psi \bar{p})$ line shape instead of a second-order polynomial function. The value of $-2\Delta \log \mathcal{L} = 80$ obtained with respect to the

nominal fit indicates that the NR($J/\psi \bar{p}$) contribution is preferred over the hypothesis of a \bar{P}_{ψ}^{N-} candidate, while consistent results for the $P_{\psi_s}^{\Lambda}(4338)^0$ state parameters are obtained. The contribution of a second narrow $P_{\psi_s}^{\Lambda 0}$ resonance is added to the nominal model to parametrize the $m(J/\psi \Lambda)$ distribution close to the $\Lambda_c^+ D_s^-$ threshold at 4255 MeV, and is found to not be statistically significant. Using the CL_s method [38], an upper limit on the $P_{\psi_s}^{\Lambda}(4255)^0$ fit fraction is set to 8.7% at a 95% confidence level. To determine the J^P assignments, all 16 combinations of $J^P = 1/2^{\pm}, 3/2^{\pm}$ are studied for the $P_{\psi_s}^{\Lambda}(4338)^0$ and NR($J/\psi \bar{p}$) spin-parity hypotheses, and those with $-2\Delta \log \mathcal{L} > 9$ with respect to the nominal fit are discarded. For the $P_{\psi_s}^{\Lambda}(4338)^0$ state, the $J^P = 3/2^{\pm}$ hypotheses are discarded, the $J^P = 1/2^-$ assignment is preferred, while the $J^P = 1/2^+$ is excluded at a 90% confidence level using the CL_s method [38].

Systematic uncertainties are evaluated on the mass and the width of the new pentaquark candidate, and on the fit fractions of $P_{\psi_s}^{\Lambda}(4338)^0$, NR($J/\psi \bar{p}$), and NR($J/\psi \Lambda$) contributions. The uncertainties are summarized in Table I and are summed in quadrature for the total contribution. For each systematic uncertainty, an ensemble of 1000 pseudoexperiments generated according to the nominal model with the same statistics as in the data is fitted with an alternative configuration that is representative of the systematic effect. The uncertainty on each parameter is determined as the mean value of the difference between the fit results of the nominal and the alternative models. The main contributions are related to the model for the decay amplitude, the bias of the fitting procedure, and the uncertainty on the reconstruction efficiency $\epsilon(m_{\bar{p}\Lambda}, \vec{Q})$. For the amplitude model, the nominal value of the hadron radius for the Blatt-Weisskopf coefficients [39] is assumed to be 3 GeV^{-1} and varied to 1 and 5 GeV^{-1} , taking the largest effect as a systematic uncertainty. Additional LS

TABLE I. Systematic uncertainties on the mass ($M_{P_{\psi_s}^{\Lambda}}$) and width ($\Gamma_{P_{\psi_s}^{\Lambda}}$) of the $P_{\psi_s}^{\Lambda 0}$ state (in MeV) and on the fit fractions $f_{P_{\psi_s}^{\Lambda}}$, $f_{\text{NR}(J/\psi \bar{p})}$, and $f_{\text{NR}(\Lambda \bar{p})}$ of the pentaquark candidate and nonresonant contributions (in %).

Source	$M_{P_{\psi_s}^{\Lambda}}$	$\Gamma_{P_{\psi_s}^{\Lambda}}$	$f_{P_{\psi_s}^{\Lambda}}$	$f_{\text{NR}(J/\psi \bar{p})}$	$f_{\text{NR}(\Lambda \bar{p})}$
Hadron radius	0.1	0.4	0.3	0.2	0.2
LS values	0.3	0.1	0.8	0.7	0.6
Breit-Wigner \bar{P}_{ψ}^{N-}	0.1	0.9	0.8
$J^P(P_{\psi_s}^{\Lambda 0})$ assignment	0.1	0.9	1.2	0.4	0.9
Fitting procedure	0.1	0.2	0.1	1.0	1.1
Efficiency	0.02	0.19	0.02	0.3	0.2
Λ decay parameters	0.02	0.04	0.01	0.3	0.2
Background	0.01	0.05	0.96	0.4	0.7
Mass resolution	0.01	0.03	0.01	0.1	0.1
Total	0.4	1.3	1.9	1.4	1.7

couplings are considered with respect to the nominal model, in particular, the $L, S = 1, 1$ ($L, S = 2, 3/2$) coupling for the production (decay) of the $P_{\psi_s}^\Lambda(4338)^0$ contribution, and the $L, S = 1, 1$ coupling for the $\text{NR}(J/\psi\bar{p})$ contribution. A relativistic Breit-Wigner function is used instead of the second-order polynomial for the line shape of the $\text{NR}(J/\psi\bar{p})$ contribution. Moreover, a model with $J^P = 1/2^+$ assignment to the $P_{\psi_s}^\Lambda(4338)^0$ state is also considered. Finally, the behavior of the maximum-likelihood estimator is studied using 1000 pseudoexperiments. Biases on the fit parameters are present due to the limited sample size and are assigned as systematic uncertainties. For the reconstruction efficiency, the nominal efficiency function based on decays from either the long or downstream Λ category and the largest effect is considered as systematic uncertainty.

Additional systematic uncertainties account for the limited knowledge of the $\Lambda \rightarrow p\pi^-$ decay amplitude parameters [30,40], the background parametrization, and the effect of the resolution on the $m(J/\psi\Lambda)$ invariant mass. The nominal background parametrization \mathcal{P}_{bkg} is obtained from the distributions of candidates in the $m(J/\psi\Lambda\bar{p})$ range $[5200, 5250] \cup [5340, 5350]$ MeV, while the parametrization obtained from the region $[5295, 5315]$ MeV is used to assess systematic effects. The background fraction $\beta = 0.07 \pm 0.01$ is also varied within uncertainties. The effect of the invariant-mass resolution, about 1 MeV on average on $m(J/\psi\Lambda)$, is estimated by smearing the invariant-mass distributions of 1000 pseudoexperiments and fitting them using the nominal model.

The mass and width of the new pentaquark candidate are measured to be $M_{P_{\psi_s}^\Lambda} = 4338.2 \pm 0.7 \pm 0.4$ MeV and $\Gamma_{P_{\psi_s}^\Lambda} = 7.0 \pm 1.2 \pm 1.3$ MeV; the measured fit fractions are $f_{P_{\psi_s}^\Lambda} = 0.125 \pm 0.007 \pm 0.019$, $f_{\text{NR}(J/\psi\bar{p})} = 0.840 \pm 0.022 \pm 0.014$, and $f_{\text{NR}(\Lambda\bar{p})} = 0.113 \pm 0.013 \pm 0.017$ for the resonant $P_{\psi_s}^\Lambda$ state, the nonresonant $\text{NR}(J/\psi\bar{p})$, and $\text{NR}(\Lambda\bar{p})$ contributions, respectively. The first uncertainty is statistical and the second systematic. The $J^P = 1/2^-$ quantum numbers for the $P_{\psi_s}^\Lambda(4338)^0$ state are preferred; $J = 1/2$ is established and positive parity can be excluded at 90% confidence level.

Because of the small Q -value of the decay, the most precise single measurement to date of the B^- mass $5279.44 \pm 0.05 \pm 0.07$ MeV is performed. This measurement is based on 1670 signal candidates with Λ baryons in the long category, which amounts to 36% of the total. Systematic uncertainties on the B^- mass include uncertainties on particle interactions with the detector material (0.030 MeV), momentum scaling due to imperfections in the magnetic-field mapping (0.039 MeV) [17], and the choice of the signal and background fit model (0.050 MeV). The alternative fit model, with compatible fit quality with respect to the nominal model, comprises an exponential function for the background and a sum of a

Gaussian and two Johnson functions for the signal. Systematic uncertainties from knowledge of the $J/\psi, \Lambda$, and p masses are negligible.

In conclusion, an amplitude analysis of the $B^- \rightarrow J/\psi\Lambda\bar{p}$ decay is performed using about 4400 signal candidates selected on data collected by the LHCb experiment between 2011 and 2018 and corresponding to an integrated luminosity of 9 fb^{-1} . A new resonant structure in the $J/\psi\Lambda$ system is found with high statistical significance, representing the first observation of a pentaquark candidate with strange quark content named the $P_{\psi_s}^\Lambda(4338)^0$ state, with spin $J = 1/2$ assigned and parity $P = -1$ preferred. The new $P_{\psi_s}^\Lambda(4338)^0$ state is found at the threshold for $\Xi_c^+ D^-$ baryon-meson production, which is relevant for the interpretation of its nature. No evidence for additional resonant states, either $P_{\psi_s}^\Lambda(4255)^0$ or \bar{P}_{ψ}^{N-} pentaquark candidates or excited K^- resonances, is found from the fit to the data.

We express our gratitude to our colleagues in the CERN accelerator departments for the excellent performance of the LHC. We thank the technical and administrative staff at the LHCb institutes. We acknowledge support from CERN and from the national agencies: CAPES, CNPq, FAPERJ, and FINEP (Brazil); MOST and NSFC (China); CNRS/IN2P3 (France); BMBF, DFG, and MPG (Germany); INFN (Italy); NWO (Netherlands); MNiSW and NCN (Poland); MEN/IFA (Romania); MICINN (Spain); SNSF and SER (Switzerland); NASU (Ukraine); STFC (United Kingdom); DOE NP, and NSF (USA). We acknowledge the computing resources that are provided by CERN, IN2P3 (France), KIT and DESY (Germany), INFN (Italy), SURF (Netherlands), PIC (Spain), GridPP (United Kingdom), CSCS (Switzerland), IFIN-HH (Romania), CBPF (Brazil), Polish WLCG (Poland) and NERSC (USA). We are indebted to the communities behind the multiple open-source software packages on which we depend. Individual groups or members have received support from ARC and ARDC (Australia); Minciencias (Colombia); AvH Foundation (Germany); EPLANET, Marie Skłodowska-Curie Actions, and ERC (European Union); A*MIDEX, ANR, IPhU, and Labex P2IO, and Région Auvergne-Rhône-Alpes (France); Key Research Program of Frontier Sciences of CAS, CAS PIFI, CAS CCEPP, Fundamental Research Funds for the Central Universities, and Science and Technology Program of Guangzhou (China); GVA, XuntaGal, GENCAT, and Prog. Atracción Talento, CM (Spain); SRC (Sweden); the Leverhulme Trust, the Royal Society, and UKRI (United Kingdom).

-
- [1] R. Aaij *et al.* (LHCb Collaboration), *Phys. Rev. Lett.* **115**, 072001 (2015).
 [2] R. Aaij *et al.* (LHCb Collaboration), *Phys. Rev. Lett.* **122**, 222001 (2019).

- [3] T. Gershon (LHCb Collaboration), Report No. CERN-LHCb-PUB-2022-013, 2022.
- [4] R. Aaij *et al.* (LHCb Collaboration), *Phys. Rev. Lett.* **122**, 191804 (2019).
- [5] R. Aaij *et al.* (LHCb Collaboration), *Phys. Rev. Lett.* **128**, 062001 (2022).
- [6] R. Aaij *et al.* (LHCb Collaboration), *Sci. Bull.* **66**, 1278 (2021).
- [7] A. Esposito, A. Pilloni, and A. D. Polosa, *Phys. Rep.* **668**, 1 (2017).
- [8] J.-M. Richard, *Few Body Syst.* **57**, 1185 (2016).
- [9] X.-K. Dong, F.-K. Guo, and B.-S. Zou, *Progr. Phys.* **41**, 65 (2021).
- [10] F.-K. Guo, C. Hanhart, Ulf-G. Meißner, Q. Wang, Q. Zhao, and B.-S. Zou, *Rev. Mod. Phys.* **90**, 015004 (2018); **94**, 029901(E) (2022).
- [11] F.-K. Guo, X.-H. Liu, and S. Sakai, *Prog. Part. Nucl. Phys.* **112**, 103757 (2020).
- [12] C. W. Xiao, J. Nieves, and E. Oset, *Phys. Lett. B* **799**, 135051 (2019).
- [13] B. Wang, L. Meng, and S.-L. Zhu, *Phys. Rev. D* **101**, 034018 (2020).
- [14] A. Ali, I. Ahmed, M. Jamil Aslam, A. Ya. Parkhomenko, and A. Rehman, *J. High Energy Phys.* **10** (2019) 256.
- [15] S. L. Olsen, T. Skwarnicki, and D. Zieminska, *Rev. Mod. Phys.* **90**, 015003 (2018).
- [16] A. M. Sirunyan *et al.* (CMS Collaboration), *J. High Energy Phys.* **12** (2019) 100.
- [17] R. Aaij *et al.* (LHCb Collaboration), *Int. J. Mod. Phys. A* **30**, 1530022 (2015).
- [18] R. Aaij *et al.*, *J. Instrum.* **9**, P09007 (2014).
- [19] R. Arink *et al.*, *J. Instrum.* **9**, P01002 (2014).
- [20] A. A. Alves, Jr. *et al.*, *J. Instrum.* **8**, P02022 (2013).
- [21] R. Aaij *et al.*, *J. Instrum.* **8**, P04022 (2013).
- [22] T. Sjöstrand, S. Mrenna, and P. Skands, *Comput. Phys. Commun.* **178**, 852 (2008).
- [23] I. Belyaev *et al.*, *J. Phys. Conf. Ser.* **331**, 032047 (2011).
- [24] D. J. Lange, *Nucl. Instrum. Methods Phys. Res., Sect. A* **462**, 152 (2001).
- [25] N. Davidson, T. Przedzinski, and Z. Was, *Comput. Phys. Commun.* **199**, 86 (2016).
- [26] J. Allison *et al.* (Geant4 Collaboration), *IEEE Trans. Nucl. Sci.* **53**, 270 (2006).
- [27] S. Agostinelli *et al.* (Geant4 Collaboration), *Nucl. Instrum. Methods Phys. Res., Sect. A* **506**, 250 (2003).
- [28] M. Clemencic, G. Corti, S. Easo, C R Jones, S. Miglioranza, M. Pappagallo, and P. Robbe, *J. Phys. Conf. Ser.* **331**, 032023 (2011).
- [29] W. D. Hulsbergen, *Nucl. Instrum. Methods Phys. Res., Sect. A* **552**, 566 (2005).
- [30] R. L. Workman *et al.* (Particle Data Group), *Prog. Theor. Exp. Phys.* **2022**, 083C01 (2022).
- [31] R. Aaij *et al.*, *Eur. Phys. J. Tech. Instrum.* **6**, 1 (2018).
- [32] L. Breiman, J. H. Friedman, R. A. Olshen, and C. J. Stone, *Classification and Regression Trees* (Wadsworth International Group, Belmont, California, 1984).
- [33] N. L. Johnson, *Biometrika* **36**, 149 (1949).
- [34] T. Skwarnicki, A study of the radiative cascade transitions between the Upsilon-prime and Upsilon resonances, Ph.D. thesis, Institute of Nuclear Physics, Krakow, 1986 [Report No. DESY-F31-86-02].
- [35] S. U. Chung, *Spin Formalisms* (CERN, Geneva, 1971), 10.5170/CERN-1971-008.
- [36] M. Mikhasenko *et al.* (JPAC Collaboration), *Phys. Rev. D* **101**, 034033 (2020).
- [37] See Supplemental Material at <http://link.aps.org/supplemental/10.1103/PhysRevLett.131.031901> for details on the amplitude model, the event-by-event efficiency parameterisation, the fit results of the nominal model, the test with angular moments, and the efficiency corrected and background subtracted distributions.
- [38] A. L. Read, *J. Phys. G* **28**, 2693 (2002).
- [39] J. M. Blatt and V. F. Weisskopf, *Theoretical Nuclear Physics* (Springer, New York, 1952).
- [40] M. Ablikim *et al.* (BESIII Collaboration), *Nat. Phys.* **15**, 631 (2019).

R. Aaij³², A. S. W. Abdelmotteleb⁵⁰, C. Abellan Beteta⁴⁴, F. Abudinén⁵⁰, T. Ackernley⁵⁴, B. Adeva⁴⁰, M. Adinolfi⁴⁸, P. Adlarson⁷⁷, H. Afsharnia⁹, C. Agapopoulou¹³, C. A. Aidala⁷⁸, Z. Ajaltouni⁹, S. Akar⁵⁹, K. Akiba³², J. Albrecht¹⁵, F. Alessio⁴², M. Alexander⁵³, A. Alfonso Albero³⁹, Z. Aliouche⁵⁶, P. Alvarez Cartelle⁴⁹, R. Amalric¹³, S. Amato², J. L. Amey⁴⁸, Y. Amhis^{11,42}, L. An⁴², L. Anderlini²², M. Andersson⁴⁴, A. Andreianov³⁸, M. Andreotti²¹, D. Andreou⁶², D. Ao⁶, F. Archilli¹⁷, A. Artamonov³⁸, M. Artuso⁶², E. Aslanides¹⁰, M. Atzeni⁴⁴, B. Audurier¹², S. Bachmann¹⁷, M. Bachmayer⁴³, J. J. Back⁵⁰, A. Bailly-reyre¹³, P. Baladron Rodriguez⁴⁰, V. Balagura¹², W. Baldini²¹, J. Baptista de Souza Leite¹, M. Barbetti^{22,b}, R. J. Barlow⁵⁶, S. Barsuk¹¹, W. Barter⁵⁵, M. Bartolini⁴⁹, F. Baryshnikov³⁸, J. M. Basels¹⁴, G. Bassi^{29,c}, B. Batsukh⁴, A. Battig¹⁵, A. Bay⁴³, A. Beck⁵⁰, M. Becker¹⁵, F. Bedeschi²⁹, I. B. Bediaga¹, A. Beiter⁶², V. Belavin³⁸, S. Belin⁴⁰, V. Bellee⁴⁴, K. Belous³⁸, I. Belov³⁸, I. Belyaev³⁸, G. Benane¹⁰, G. Bencivenni²³, E. Ben-Haim¹³, A. Berezhnoy³⁸, R. Bernet⁴⁴, S. Bernet Andres⁷⁶, D. Berninghoff¹⁷, H. C. Bernstein⁶², C. Bertella⁵⁶, A. Bertolin²⁸, C. Betancourt⁴⁴, F. Betti⁴², Ia. Bezshyiko⁴⁴, S. Bhasin⁴⁸, J. Bhom³⁵, L. Bian⁶⁸, M. S. Bieker¹⁵, N. V. Biesuz²¹, S. Bifani⁴⁷, P. Billoir¹³, A. Biolchini³², M. Birch⁵⁵, F. C. R. Bishop⁴⁹, A. Bitadze⁵⁶, A. Bizzeti¹⁵, M. P. Blago⁴⁹, T. Blake⁵⁰, F. Blanc⁴³, J. E. Blank¹⁵, S. Blusk⁶², D. Bobulska⁵³, J. A. Boelhauve¹⁵, O. Boente Garcia¹², T. Boettcher⁵⁹, A. Boldyrev³⁸, C. S. Bolognani⁷⁴

R. Bolzonella^{21,d}, N. Bondar^{38,42}, F. Borgato²⁸, S. Borghi⁵⁶, M. Borsato¹⁷, J. T. Borsuk³⁵, S. A. Bouchiba⁴³, T. J. V. Bowcock⁵⁴, A. Boyer⁴², C. Bozzi²¹, M. J. Bradley⁵⁵, S. Braun⁶⁰, A. Brea Rodriguez⁴⁰, J. Brodzicka³⁵, A. Brossa Gonzalo⁴⁰, J. Brown⁵⁴, D. Brundu²⁷, A. Buonaura⁴⁴, L. Buonincontri²⁸, A. T. Burke⁵⁶, C. Burr⁴², A. Bursche⁶⁶, A. Butkevich³⁸, J. S. Butter³², J. Buytaert⁴², W. Byczynski⁴², S. Cadeddu²⁷, H. Cai⁶⁸, R. Calabrese^{21,d}, L. Calefice¹⁵, S. Cali²³, R. Calladine⁴⁷, M. Calvi^{26,e}, M. Calvo Gomez⁷⁶, P. Campana²³, D. H. Campora Perez⁷⁴, A. F. Campoverde Quezada⁶, S. Capelli^{26,e}, L. Capriotti²⁰, A. Carbone^{20,f}, G. Carboni³¹, R. Cardinale^{24,g}, A. Cardini²⁷, P. Carniti^{26,e}, L. Carus¹⁴, A. Casais Vidal⁴⁰, R. Caspary¹⁷, G. Casse⁵⁴, M. Cattaneo⁴², G. Cavallero⁴², V. Cavallini^{21,d}, S. Celani⁴³, J. Cerasoli¹⁰, D. Cervenkov⁵⁷, A. J. Chadwick⁵⁴, M. G. Chapman⁴⁸, M. Charles¹³, Ph. Charpentier⁴², C. A. Chavez Barajas⁵⁴, M. Chefdeville⁸, C. Chen³, S. Chen⁴, A. Chernov³⁵, S. Chernyshenko⁴⁶, V. Chobanova⁴⁰, S. Cholak⁴³, M. Chruszcz³⁵, A. Chubykin³⁸, V. Chulikov³⁸, P. Ciambrone²³, M. F. Cicala⁵⁰, X. Cid Vidal⁴⁰, G. Ciezarek⁴², G. Ciullo^{21,d}, P. E. L. Clarke⁵², M. Clemencic⁴², H. V. Cliff⁴⁹, J. Closier⁴², J. L. Cobbedick⁵⁶, V. Coco⁴², J. A. B. Coelho¹¹, J. Cogan¹⁰, E. Cogneras⁹, L. Cojocariu³⁷, P. Collins⁴², T. Colombo⁴², L. Congedo¹⁹, A. Contu²⁷, N. Cooke⁴⁷, I. Corredoira⁴⁰, G. Corti⁴², B. Couturier⁴², D. C. Craik⁴⁴, M. Cruz Torres^{1,h}, R. Currie⁵², C. L. Da Silva⁶¹, S. Dadabaev³⁸, L. Dai⁶⁵, X. Dai⁵, E. Dall'Occo¹⁵, J. Dalseno⁴⁰, C. D'Ambrosio⁴², J. Daniel⁹, A. Danilina³⁸, P. d'Argent¹⁵, J. E. Davies⁵⁶, A. Davis⁵⁶, O. De Aguiar Francisco⁵⁶, J. de Boer⁴², K. De Bruyn⁷³, S. De Capua⁵⁶, M. De Cian⁴³, U. De Freitas Carneiro Da Graca¹, E. De Lucia²³, J. M. De Miranda¹, L. De Paula², M. De Serio^{19,i}, D. De Simone⁴⁴, P. De Simone²³, F. De Vellis¹⁵, J. A. de Vries⁷⁴, C. T. Dean⁶¹, F. Debernardis^{19,i}, D. Decamp⁸, V. Dedu¹⁰, L. Del Buono¹³, B. Delaney⁵⁸, H.-P. Dembinski¹⁵, V. Denysenko⁴⁴, O. Deschamps⁹, F. Dettori^{27,j}, B. Dey⁷¹, P. Di Nezza²³, I. Diachkov³⁸, S. Didenko³⁸, L. Dieste Maronas⁴⁰, S. Ding⁶², V. Dobishuk⁴⁶, A. Dolmatov³⁸, C. Dong³, A. M. Donohoe¹⁸, F. Dordei²⁷, A. C. dos Reis¹, L. Douglas⁵³, A. G. Downes⁸, P. Duda⁷⁵, M. W. Dudek³⁵, L. Dufour⁴², V. Duk⁷², P. Durante⁴², M. M. Duras⁷⁵, J. M. Durham⁶¹, D. Dutta⁵⁶, A. Dziurda³⁵, A. Dzyuba³⁸, S. Easo⁵¹, U. Egede⁶³, V. Egorychev³⁸, S. Eidelman^{38,a}, C. Eirea Orro⁴⁰, S. Eisenhardt⁵², E. Ejopu⁵⁶, S. Ek-In⁴³, L. Eklund⁷⁷, S. Ely⁶², A. Ene³⁷, E. Epple⁵⁹, S. Escher¹⁴, J. Eschle⁴⁴, S. Esen⁴⁴, T. Evans⁵⁶, F. Fabiano^{27,j}, L. N. Falcao¹, Y. Fan⁶, B. Fang^{11,68}, L. Fantini^{72,k}, M. Faria⁴³, S. Farry⁵⁴, D. Fazzini^{26,e}, L. F. Felkowski⁷⁵, M. Feo⁴², M. Fernandez Gomez⁴⁰, A. D. Fernandez⁶⁰, F. Ferrari²⁰, L. Ferreira Lopes⁴³, F. Ferreira Rodrigues², S. Ferreres Sole³², M. Ferrillo⁴⁴, M. Ferro-Luzzi⁴², S. Filippov³⁸, R. A. Fini¹⁹, M. Fiorini^{21,d}, M. Firlej³⁴, K. M. Fischer⁵⁷, D. S. Fitzgerald⁷⁸, C. Fitzpatrick⁵⁶, T. Fiutowski³⁴, F. Fleuret¹², M. Fontana¹³, F. Fontanelli^{24,g}, R. Forty⁴², D. Foulds-Holt⁴⁹, V. Franco Lima⁵⁴, M. Franco Sevilla⁶⁰, M. Frank⁴², E. Franzoso^{21,d}, G. Frau¹⁷, C. Frei⁴², D. A. Friday⁵³, J. Fu⁶, Q. Fuehring¹⁵, T. Fulghesu¹³, E. Gabriel³², G. Galati^{19,i}, M. D. Galati³², A. Gallas Torreira⁴⁰, D. Galli^{20,f}, S. Gambetta^{52,42}, Y. Gan³, M. Gandelman², P. Gandini²⁵, Y. Gao⁷, Y. Gao⁵, M. Garau^{27,j}, L. M. Garcia Martin⁵⁰, P. Garcia Moreno³⁹, J. Garcia Pardiñas^{26,e}, B. Garcia Plana⁴⁰, F. A. Garcia Rosales¹², L. Garrido³⁹, C. Gaspar⁴², R. E. Geertsema³², D. Gerick¹⁷, L. L. Gerken¹⁵, E. Gersabeck⁵⁶, M. Gersabeck⁵⁶, T. Gershon⁵⁰, L. Giambastiani²⁸, V. Gibson⁴⁹, H. K. Gienza³⁶, A. L. Gilman⁵⁷, M. Giovannetti^{23,l}, A. Gioventù⁴⁰, P. Gironella Gironell³⁹, C. Giugliano^{21,d}, M. A. Giza³⁵, K. Gizdov⁵², E. L. Gkougkousis⁴², V. V. Gligorov^{13,42}, C. Göbel⁶⁴, E. Golobardes⁷⁶, D. Golubkov³⁸, A. Golutvin^{55,38}, A. Gomes^{1,m}, S. Gomez Fernandez³⁹, F. Goncalves Abrantes⁵⁷, M. Goncerz³⁵, G. Gong³, I. V. Gorelov³⁸, C. Gotti²⁶, J. P. Grabowski⁷⁰, T. Grammatico¹³, L. A. Granado Cardoso⁴², E. Graugés³⁹, E. Graverini⁴³, G. Graziani⁴³, A. T. Grecu³⁷, L. M. Greeven³², N. A. Grieser⁴, L. Grillo⁵³, S. Gromov³⁸, B. R. Gruberg Cazon⁵⁷, C. Gu³, M. Guarise^{21,d}, M. Guittiere¹¹, P. A. Günther¹⁷, E. Gushchin³⁸, A. Guth¹⁴, Y. Guz³⁸, T. Gys⁴², T. Hadavizadeh⁶³, C. Hadjivasiliou⁶⁰, G. Haefeli⁴³, C. Haen⁴², J. Haimberger⁴², S. C. Haines⁴⁹, T. Halewood-leagas⁵⁴, M. M. Halvorsen⁴², P. M. Hamilton⁶⁰, J. Hammerich⁵⁴, Q. Han⁷, X. Han¹⁷, E. B. Hansen⁵⁶, S. Hansmann-Menzemer¹⁷, L. Hao⁶, N. Harnew⁵⁷, T. Harrison⁵⁴, C. Hasse⁴², M. Hatch⁴², J. He^{6,n}, K. Heijhoff³², C. Henderson⁵⁹, R. D. L. Henderson^{63,50}, A. M. Hennequin⁵⁸, K. Hennessy⁵⁴, L. Henry⁴², J. Herd⁵⁵, J. Heuel¹⁴, A. Hicheur², D. Hill⁴³, M. Hilton⁵⁶, S. E. Hollitt¹⁵, J. Horswill⁵⁶, R. Hou⁷, Y. Hou⁸, J. Hu¹⁷, J. Hu⁶⁶, W. Hu⁵, X. Hu³, W. Huang⁶, X. Huang⁶⁸, W. Hulsbergen³², R. J. Hunter⁵⁰, M. Hushchyn³⁸, D. Hutchcroft⁵⁴, P. Ibis¹⁵, M. Idzik³⁴, D. Ilin³⁸, P. Ilten⁵⁹, A. Inglessi³⁸, A. Iniukhin³⁸, A. Ishteev³⁸, K. Ivshin³⁸, R. Jacobsson⁴², H. Jage¹⁴, S. J. Jaimes Elles⁴¹, S. Jakobsen⁴², E. Jans³², B. K. Jashal⁴¹

A. Jawahery⁶⁰, V. Jevtic¹⁵, E. Jiang⁶⁰, X. Jiang^{4,6}, Y. Jiang⁶, M. John⁵⁷, D. Johnson⁵⁸, C. R. Jones⁴⁹, T. P. Jones⁵⁰, B. Jost⁴², N. Jurik⁴², I. Juszczak³⁵, S. Kandybei⁴⁵, Y. Kang³, M. Karacson⁴², D. Karpenkov³⁸, M. Karpov³⁸, J. W. Kautz⁵⁹, F. Keizer⁴², D. M. Keller⁶², M. Kenzie⁵⁰, T. Ketel³², B. Khanji¹⁵, A. Kharisova³⁸, S. Kholodenko³⁸, G. Khreich¹¹, T. Kim¹⁴, V. S. Kirsebom⁴³, O. Kitouni⁵⁸, S. Klaver³³, N. Kleijne^{29,c}, K. Klimaszewski³⁶, M. R. Kmiec³⁶, S. Koliiev⁴⁶, A. Kondybayeva³⁸, A. Konoplyannikov³⁸, P. Kopciwicz³⁴, R. Kopečna¹⁷, P. Koppenburg³², M. Korolev³⁸, I. Kostiuk^{32,46}, O. Kot⁴⁶, S. Kotriakhova¹⁰, A. Kozachuk³⁸, P. Kravchenko³⁸, L. Kravchuk³⁸, R. D. Krawczyk⁴², M. Kreps⁵⁰, S. Kretzschmar¹⁴, P. Krokovny³⁸, W. Krupa³⁴, W. Krzemien³⁶, J. Kubat¹⁷, S. Kubis⁷⁵, W. Kucewicz^{35,34}, M. Kucharczyk³⁵, V. Kudryavtsev³⁸, A. Kupsc⁷⁷, D. Lacarrere⁴², G. Lafferty⁵⁶, A. Lai²⁷, A. Lampis^{27,j}, D. Lancierini⁴⁴, C. Landesa Gomez⁴⁰, J. J. Lane⁵⁶, R. Lane⁴⁸, G. Lanfranchi²³, C. Langenbruch¹⁴, J. Langer¹⁵, O. Lantwin³⁸, T. Latham⁵⁰, F. Lazzari^{29,o}, M. Lazzaroni^{25,p}, R. Le Gac¹⁰, S. H. Lee⁷⁸, R. Lefèvre⁹, A. Leflat³⁸, S. Legotin³⁸, P. Lenisa^{21,d}, O. Leroy¹⁰, T. Lesiak³⁵, B. Leverington¹⁷, A. Li³, H. Li⁶⁶, K. Li⁷, P. Li¹⁷, P.-R. Li⁶⁷, S. Li⁷, T. Li⁴, T. Li⁶⁶, Y. Li⁴, Z. Li⁶², X. Liang⁶², C. Lin⁶, T. Lin⁵¹, R. Lindner⁴², V. Lisovskyi¹⁵, R. Litvinov^{27,j}, G. Liu⁶⁶, H. Liu⁶, Q. Liu⁶, S. Liu^{4,6}, A. Lobo Salvia³⁹, A. Loi²⁷, R. Lollini⁷², J. Lomba Castro⁴⁰, I. Longstaff⁵³, J. H. Lopes², A. Lopez Huertas³⁹, S. López Soliño⁴⁰, G. H. Lovell⁴⁹, Y. Lu^{4,q}, C. Lucarelli^{22,b}, D. Lucchesi^{28,r}, S. Luchuk³⁸, M. Lucio Martinez⁷⁴, V. Lukashenko^{32,46}, Y. Luo³, A. Lupato⁵⁶, E. Luppi^{21,d}, A. Lusiani^{29,c}, K. Lynch¹⁸, X.-R. Lyu⁶, L. Ma⁴, R. Ma⁶, S. Maccolini²⁰, F. Machefert¹¹, F. Maciuc³⁷, I. Mackay⁵⁷, V. Macko⁴³, P. Mackowiak¹⁵, L. R. Madhan Mohan⁴⁸, A. Maevskiy³⁸, D. Maisuzenko³⁸, M. W. Majewski³⁴, J. J. Malczewski³⁵, S. Malde⁵⁷, B. Malecki^{35,42}, A. Malinin³⁸, T. Maltsev³⁸, G. Manca^{27,j}, G. Mancinelli¹⁰, C. Mancuso^{11,25,p}, D. Manuzzi²⁰, C. A. Manzari⁴⁴, D. Marangotto^{25,p}, J. F. Marchand⁸, U. Marconi²⁰, S. Mariani^{22,b}, C. Marin Benito³⁹, J. Marks¹⁷, A. M. Marshall⁴⁸, P. J. Marshall⁵⁴, G. Martelli^{72,k}, G. Martellotti³⁰, L. Martinazzoli^{42,e}, M. Martinelli^{26,e}, D. Martinez Santos⁴⁰, F. Martinez Vidal⁴¹, A. Massafferri¹, M. Materok¹⁴, R. Matev⁴², A. Mathad⁴⁴, V. Matiunin³⁸, C. Matteuzzi²⁶, K. R. Mattioli¹², A. Mauri³², E. Maurice¹², J. Mauricio³⁹, M. Mazurek⁴², M. McCann⁵⁵, L. Mcconnell¹⁸, T. H. McGrath⁵⁶, N. T. McHugh⁵³, A. McNab⁵⁶, R. McNulty¹⁸, J. V. Mead⁵⁴, B. Meadows⁵⁹, G. Meier¹⁵, D. Melnychuk³⁶, S. Meloni^{26,e}, M. Merk^{32,74}, A. Merli^{25,p}, L. Meyer Garcia², D. Miao^{4,6}, M. Mikhasenko^{70,s}, D. A. Milanes⁶⁹, E. Millard⁵⁰, M. Milovanovic⁴², M.-N. Minard^{8,a}, A. Minotti^{26,e}, T. Miralles⁹, S. E. Mitchell⁵², B. Mitreska⁵⁶, D. S. Mitzel¹⁵, A. Mödden¹⁵, R. A. Mohammed⁵⁷, R. D. Moise¹⁴, S. Mokhnenko³⁸, T. Mombächer⁴⁰, M. Monk^{50,63}, I. A. Monroy⁶⁹, S. Monteil⁹, M. Morandin²⁸, G. Morello²³, M. J. Morello^{29,c}, J. Moron³⁴, A. B. Morris⁷⁰, A. G. Morris⁵⁰, R. Mountain⁶², H. Mu³, E. Muhammad⁵⁰, F. Muheim⁵², M. Mulder⁷³, K. Müller⁴⁴, C. H. Murphy⁵⁷, D. Murray⁵⁶, R. Murta⁵⁵, P. Muzzetto^{27,j}, P. Naik⁴⁸, T. Nakada⁴³, R. Nandakumar⁵¹, T. Nanut⁴², I. Nasteva², M. Needham⁵², N. Neri^{25,p}, S. Neubert⁷⁰, N. Neufeld⁴², P. Neustroev³⁸, R. Newcombe⁵⁵, J. Nicolini^{15,11}, E. M. Niel⁴³, S. Nieswand¹⁴, N. Nikitin³⁸, N. S. Nolte⁵⁸, C. Normand^{8,27,j}, J. Novoa Fernandez⁴⁰, C. Nunez⁷⁸, A. Oblakowska-Mucha³⁴, V. Obraztsov³⁸, T. Oeser¹⁴, D. P. O'Hanlon⁴⁸, S. Okamura^{21,d}, R. Oldeman^{27,j}, F. Oliva⁵², C. J. G. Onderwater⁷³, R. H. O'Neil⁵², J. M. Otalora Goicochea², T. Ovsianikova³⁸, P. Owen⁴⁴, A. Oyanguren⁴¹, O. Ozcelik⁵², K. O. Padeken⁷⁰, B. Pagare⁵⁰, P. R. Pais⁴², T. Pajero⁵⁷, A. Palano¹⁹, M. Palutan²³, Y. Pan⁵⁶, G. Panshin³⁸, L. Paolucci⁵⁰, A. Papanestis⁵¹, M. Pappagallo^{19,i}, L. L. Pappalardo^{21,d}, C. Pappenheimer⁵⁹, W. Parker⁶⁰, C. Parkes⁵⁶, B. Passalacqua^{21,d}, G. Passaleva²², A. Pastore¹⁹, M. Patel⁵⁵, C. Patrignani^{20,f}, C. J. Pawley⁷⁴, A. Pearce⁴², A. Pellegrino³², M. Pepe Altarelli⁴², S. Perazzini²⁰, D. Pereima³⁸, A. Pereiro Castro⁴⁰, P. Perret⁹, M. Petric⁵³, K. Petridis⁴⁸, A. Petrolini^{24,g}, A. Petrov³⁸, S. Petrucci⁵², M. Petruzzo²⁵, H. Pham⁶², A. Philippov³⁸, R. Piandani⁶, L. Pica^{29,c}, M. Piccini⁷², B. Pietrzyk⁸, G. Pietrzyk¹¹, M. Pili⁵⁷, A. Pilloni^{62,t}, D. Pinci³⁰, F. Pisani⁴², M. Pizzichemi^{26,42,e}, V. Placinta³⁷, J. Plews⁴⁷, M. Plo Casasus⁴⁰, F. Polci^{13,42}, M. Poli Lener²³, M. Poliakov⁶², A. Poluektov¹⁰, N. Polukhina³⁸, I. Polyakov⁴², E. Polycarpo², S. Ponce⁴², D. Popov^{6,42}, S. Popov³⁸, S. Poslavskii³⁸, K. Prasanth³⁵, L. Promberger¹⁷, C. Prouve⁴⁰, V. Pugatch⁴⁶, V. Puill¹¹, G. Punzi^{29,u}, H. R. Qi³, W. Qian⁶, N. Qin³, S. Qu³, R. Quagliani⁴³, N. V. Raab¹⁸, R. I. Rabadan Trejo⁶, B. Rachwal³⁴, J. H. Rademacker⁴⁸, R. Rajagopalan⁶², M. Rama²⁹, M. Ramos Pernas⁵⁰, M. S. Rangel², F. Ratnikov³⁸, G. Raven^{33,42}, M. Rebollo De Miguel⁴¹, F. Redi⁴², J. Reich⁴⁸, F. Reiss⁵⁶, C. Remon Alepuz⁴¹, Z. Ren³, P. K. Resmi¹⁰, R. Ribatti^{29,c}, A. M. Ricci²⁷, S. Ricciardi⁵¹, K. Richardson⁵⁸, M. Richardson-Slipper⁵², K. Rinnert⁵⁴, P. Robbe¹¹, G. Robertson⁵², A. B. Rodrigues⁴³, E. Rodrigues⁵⁴

E. Rodriguez Fernandez⁴⁰, J. A. Rodriguez Lopez⁶⁹, E. Rodriguez Rodriguez⁴⁰, D. L. Rolf⁴², A. Rollings⁵⁷, P. Roloff⁴², V. Romanovskiy³⁸, M. Romero Lamas⁴⁰, A. Romero Vidal⁴⁰, J. D. Roth^{78,a}, M. Rotondo²³, M. S. Rudolph⁶², T. Ruf⁴², R. A. Ruiz Fernandez⁴⁰, J. Ruiz Vidal⁴¹, A. Ryzhikov³⁸, J. Ryzka³⁴, J. J. Saborido Silva⁴⁰, N. Sagidova³⁸, N. Sahoo⁴⁷, B. Saitta^{27,j}, M. Salomoni⁴², C. Sanchez Gras³², I. Sanderswood⁴¹, R. Santacesaria³⁰, C. Santamarina Rios⁴⁰, M. Santimaria²³, E. Santovetti^{31,l}, D. Saranin³⁸, G. Sarpis¹⁴, M. Sarpis⁷⁰, A. Sarti³⁰, C. Satriano^{30,v}, A. Satta³¹, M. Saur¹⁵, D. Savrina³⁸, H. Sazak⁹, L. G. Scantlebury Smead⁵⁷, A. Scarabotto¹³, S. Schael¹⁴, S. Scherl⁵⁴, M. Schiller⁵³, H. Schindler⁴², M. Schmelling¹⁶, B. Schmidt⁴², S. Schmitt¹⁴, O. Schneider⁴³, A. Schopper⁴², M. Schubiger³², S. Schulte⁴³, M. H. Schune¹¹, R. Schwemmer⁴², B. Sciascia^{23,42}, A. Sciuccati⁴², S. Sellam⁴⁰, A. Semennikov³⁸, M. Senghi Soares³³, A. Sergi^{24,g}, N. Serra⁴⁴, L. Sestini²⁸, A. Seuthe¹⁵, Y. Shang⁵, D. M. Shangase⁷⁸, M. Shapkin³⁸, I. Shchemerov³⁸, L. Shchutska⁴³, T. Shears⁵⁴, L. Shekhtman³⁸, Z. Shen⁵, S. Sheng^{4,6}, V. Shevchenko³⁸, B. Shi⁶, E. B. Shields^{26,e}, Y. Shimizu¹¹, E. Shmanin³⁸, R. Shorkin³⁸, J. D. Shupperd⁶², B. G. Siddi^{21,d}, R. Silva Coutinho⁶², G. Simi²⁸, S. Simone^{19,i}, M. Singla⁶³, N. Skidmore⁵⁶, R. Skuza¹⁷, T. Skwarnicki⁶², M. W. Slater⁴⁷, J. C. Smallwood⁵⁷, J. G. Smeaton⁴⁹, E. Smith⁴⁴, K. Smith⁶¹, M. Smith⁵⁵, A. Snoch³², L. Soares Lavra⁹, M. D. Sokoloff⁵⁹, F. J. P. Soler⁵³, A. Solomin^{38,48}, A. Solovev³⁸, I. Solovyev³⁸, R. Song⁶³, F. L. Souza De Almeida², B. Souza De Paula², B. Spaan^{15,a}, E. Spadaro Norella^{25,p}, E. Spedicato²⁰, E. Spiridenkov³⁸, P. Spradlin⁵³, V. Sriskaran⁴², F. Stagni⁴², M. Stahl⁴², S. Stahl⁴², S. Stanislaus⁵⁷, E. N. Stein⁴², O. Steinkamp⁴⁴, O. Stenyakin³⁸, H. Stevens¹⁵, S. Stone^{62,a}, D. Strelakina³⁸, Y. S. Su⁶, F. Suljik⁵⁷, J. Sun²⁷, L. Sun⁶⁸, Y. Sun⁶⁰, P. Svihra⁵⁶, P. N. Swallow⁴⁷, K. Swientek³⁴, A. Szabelski³⁶, T. Szumlak³⁴, M. Szymanski⁴², Y. Tan³, S. Taneja⁵⁶, M. D. Tat⁵⁷, A. Terentev³⁸, F. Teubert⁴², E. Thomas⁴², D. J. D. Thompson⁴⁷, K. A. Thomson⁵⁴, H. Tilquin⁵⁵, V. Tisserand⁹, S. T'Jampens⁸, M. Tobin⁴, L. Tomassetti^{21,d}, G. Tonani^{25,p}, X. Tong⁵, D. Torres Machado¹, D. Y. Tou³, S. M. Trilov⁴⁸, C. Trippl⁴³, G. Tuci⁶, A. Tully⁴³, N. Tuning³², A. Ukleja³⁶, D. J. Unverzagt¹⁷, A. Usachov³², A. Ustyuzhanin³⁸, U. Uwer¹⁷, A. Vagner³⁸, V. Vagnoni²⁰, A. Valassi⁴², G. Valenti²⁰, N. Valls Canudas⁷⁶, M. van Beuzekom³², M. Van Dijk⁴³, H. Van Hecke⁶¹, E. van Herwijnen⁵⁵, C. B. Van Hulse^{40,w}, M. van Veghel⁷³, R. Vazquez Gomez³⁹, P. Vazquez Regueiro⁴⁰, C. Vázquez Sierra⁴², S. Vecchi²¹, J. J. Velthuis⁴⁸, M. Veltri^{22,x}, A. Venkateswaran⁴³, M. Veronesi³², M. Vesterinen⁵⁰, D. Vieira⁵⁹, M. Vieites Diaz⁴³, X. Vilasis-Cardona⁷⁶, E. Vilella Figueras⁵⁴, A. Villa²⁰, P. Vincent¹³, F. C. Volle¹¹, D. vom Bruch¹⁰, A. Vorobyev³⁸, V. Vorobyev³⁸, N. Voropaev³⁸, K. Vos⁷⁴, C. Vrahas⁵², R. Waldi¹⁷, J. Walsh²⁹, G. Wan⁵, C. Wang¹⁷, G. Wang⁷, J. Wang⁵, J. Wang⁴, J. Wang³, J. Wang⁶⁸, M. Wang⁵, R. Wang⁴⁸, X. Wang⁶⁶, Y. Wang⁷, Z. Wang⁴⁴, Z. Wang³, Z. Wang⁶, J. A. Ward^{50,63}, N. K. Watson⁴⁷, D. Websdale⁵⁵, Y. Wei⁵, C. Weisser⁵⁸, B. D. C. Westhenry⁴⁸, D. J. White⁵⁶, M. Whitehead⁵³, A. R. Wiederhold⁵⁰, D. Wiedner¹⁵, G. Wilkinson⁵⁷, M. K. Wilkinson⁵⁹, I. Williams⁴⁹, M. Williams⁵⁸, M. R. J. Williams⁵², R. Williams⁴⁹, F. F. Wilson⁵¹, W. Wislicki³⁶, M. Witek³⁵, L. Witola¹⁷, C. P. Wong⁶¹, G. Wormser¹¹, S. A. Wotton⁴⁹, H. Wu⁶², J. Wu⁷, K. Wyllie⁴², Z. Xiang⁶, D. Xiao⁷, Y. Xie⁷, A. Xu⁵, J. Xu⁶, L. Xu³, L. Xu³, M. Xu⁵⁰, Q. Xu⁶, Z. Xu⁹, Z. Xu⁶, D. Yang³, S. Yang⁶, X. Yang⁵, Y. Yang⁶, Z. Yang⁵, Z. Yang⁶⁰, L. E. Yeomans⁵⁴, V. Yeroshenko¹¹, H. Yeung⁵⁶, H. Yin⁷, J. Yu⁶⁵, X. Yuan⁶², E. Zaffaroni⁴³, M. Zavertyaev¹⁶, M. Zdybal³⁵, O. Zenaiev⁴², M. Zeng³, C. Zhang⁵, D. Zhang⁷, L. Zhang³, S. Zhang⁶⁵, S. Zhang⁵, Y. Zhang⁵, Y. Zhang⁵⁷, A. Zharkova³⁸, A. Zhelezov¹⁷, Y. Zheng⁶, T. Zhou⁵, X. Zhou⁶, Y. Zhou⁶, V. Zhovkovska¹¹, X. Zhu³, X. Zhu⁷, Z. Zhu⁶, V. Zhukov^{14,38}, Q. Zou^{4,6}, S. Zucchelli^{20,f}, D. Zuliani²⁸ and G. Zunica⁵⁶

(LHCb Collaboration)

¹Centro Brasileiro de Pesquisas Físicas (CBPF), Rio de Janeiro, Brazil²Universidade Federal do Rio de Janeiro (UFRJ), Rio de Janeiro, Brazil³Center for High Energy Physics, Tsinghua University, Beijing, China⁴Institute Of High Energy Physics (IHEP), Beijing, China⁵School of Physics State Key Laboratory of Nuclear Physics and Technology, Peking University, Beijing, China⁶University of Chinese Academy of Sciences, Beijing, China

- ⁷*Institute of Particle Physics, Central China Normal University, Wuhan, Hubei, China*
- ⁸*Université Savoie Mont Blanc, CNRS, IN2P3-LAPP, Annecy, France*
- ⁹*Université Clermont Auvergne, CNRS/IN2P3, LPC, Clermont-Ferrand, France*
- ¹⁰*Aix Marseille Univ, CNRS/IN2P3, CPPM, Marseille, France*
- ¹¹*Université Paris-Saclay, CNRS/IN2P3, IJCLab, Orsay, France*
- ¹²*Laboratoire Leprince-Ringuet, CNRS/IN2P3, Ecole Polytechnique, Institut Polytechnique de Paris, Palaiseau, France*
- ¹³*LPNHE, Sorbonne Université, Paris Diderot Sorbonne Paris Cité, CNRS/IN2P3, Paris, France*
- ¹⁴*I. Physikalisches Institut, RWTH Aachen University, Aachen, Germany*
- ¹⁵*Fakultät Physik, Technische Universität Dortmund, Dortmund, Germany*
- ¹⁶*Max-Planck-Institut für Kernphysik (MPIK), Heidelberg, Germany*
- ¹⁷*Physikalisches Institut, Ruprecht-Karls-Universität Heidelberg, Heidelberg, Germany*
- ¹⁸*School of Physics, University College Dublin, Dublin, Ireland*
- ¹⁹*INFN Sezione di Bari, Bari, Italy*
- ²⁰*INFN Sezione di Bologna, Bologna, Italy*
- ²¹*INFN Sezione di Ferrara, Ferrara, Italy*
- ²²*INFN Sezione di Firenze, Firenze, Italy*
- ²³*INFN Laboratori Nazionali di Frascati, Frascati, Italy*
- ²⁴*INFN Sezione di Genova, Genova, Italy*
- ²⁵*INFN Sezione di Milano, Milano, Italy*
- ²⁶*INFN Sezione di Milano-Bicocca, Milano, Italy*
- ²⁷*INFN Sezione di Cagliari, Monserrato, Italy*
- ²⁸*Università degli Studi di Padova, Università e INFN, Padova, Padova, Italy*
- ²⁹*INFN Sezione di Pisa, Pisa, Italy*
- ³⁰*INFN Sezione di Roma La Sapienza, Roma, Italy*
- ³¹*INFN Sezione di Roma Tor Vergata, Roma, Italy*
- ³²*Nikhef National Institute for Subatomic Physics, Amsterdam, Netherlands*
- ³³*Nikhef National Institute for Subatomic Physics and VU University Amsterdam, Amsterdam, Netherlands*
- ³⁴*AGH—University of Science and Technology, Faculty of Physics and Applied Computer Science, Kraków, Poland*
- ³⁵*Henryk Niewodniczanski Institute of Nuclear Physics Polish Academy of Sciences, Kraków, Poland*
- ³⁶*National Center for Nuclear Research (NCBJ), Warsaw, Poland*
- ³⁷*Horia Hulubei National Institute of Physics and Nuclear Engineering, Bucharest-Magurele, Romania*
- ³⁸*Affiliated with an institute covered by a cooperation agreement with CERN*
- ³⁹*ICCUB, Universitat de Barcelona, Barcelona, Spain*
- ⁴⁰*Instituto Galego de Física de Altas Enerxías (IGFAE), Universidade de Santiago de Compostela, Santiago de Compostela, Spain*
- ⁴¹*Instituto de Física Corpuscular, Centro Mixto Universidad de Valencia—CSIC, Valencia, Spain*
- ⁴²*European Organization for Nuclear Research (CERN), Geneva, Switzerland*
- ⁴³*Institute of Physics, Ecole Polytechnique Fédérale de Lausanne (EPFL), Lausanne, Switzerland*
- ⁴⁴*Physik-Institut, Universität Zürich, Zürich, Switzerland*
- ⁴⁵*NSC Kharkiv Institute of Physics and Technology (NSC KIPT), Kharkiv, Ukraine*
- ⁴⁶*Institute for Nuclear Research of the National Academy of Sciences (KINR), Kyiv, Ukraine*
- ⁴⁷*University of Birmingham, Birmingham, United Kingdom*
- ⁴⁸*H.H. Wills Physics Laboratory, University of Bristol, Bristol, United Kingdom*
- ⁴⁹*Cavendish Laboratory, University of Cambridge, Cambridge, United Kingdom*
- ⁵⁰*Department of Physics, University of Warwick, Coventry, United Kingdom*
- ⁵¹*STFC Rutherford Appleton Laboratory, Didcot, United Kingdom*
- ⁵²*School of Physics and Astronomy, University of Edinburgh, Edinburgh, United Kingdom*
- ⁵³*School of Physics and Astronomy, University of Glasgow, Glasgow, United Kingdom*
- ⁵⁴*Oliver Lodge Laboratory, University of Liverpool, Liverpool, United Kingdom*
- ⁵⁵*Imperial College London, London, United Kingdom*
- ⁵⁶*Department of Physics and Astronomy, University of Manchester, Manchester, United Kingdom*
- ⁵⁷*Department of Physics, University of Oxford, Oxford, United Kingdom*
- ⁵⁸*Massachusetts Institute of Technology, Cambridge, Massachusetts, USA*
- ⁵⁹*University of Cincinnati, Cincinnati, Ohio, USA*
- ⁶⁰*University of Maryland, College Park, Maryland, USA*
- ⁶¹*Los Alamos National Laboratory (LANL), Los Alamos, New Mexico, USA*
- ⁶²*Syracuse University, Syracuse, New York, USA*
- ⁶³*School of Physics and Astronomy, Monash University, Melbourne, Australia
(associated with Department of Physics, University of Warwick, Coventry, United Kingdom)*

⁶⁴*Pontificia Universidade Católica do Rio de Janeiro (PUC-Rio), Rio de Janeiro, Brazil
(associated with Universidade Federal do Rio de Janeiro (UFRJ), Rio de Janeiro, Brazil)*

⁶⁵*Physics and Micro Electronic College, Hunan University, Changsha City, China
(associated with Institute of Particle Physics, Central China Normal University, Wuhan, Hubei, China)*

⁶⁶*Guangdong Provincial Key Laboratory of Nuclear Science, Guangdong-Hong Kong Joint Laboratory of Quantum Matter,
Institute of Quantum Matter, South China Normal University, Guangzhou, China
(associated with Center for High Energy Physics, Tsinghua University, Beijing, China)*

⁶⁷*Lanzhou University, Lanzhou, China
(associated with Institute Of High Energy Physics (IHEP), Beijing, China)*

⁶⁸*School of Physics and Technology, Wuhan University, Wuhan, China
(associated with Center for High Energy Physics, Tsinghua University, Beijing, China)*

⁶⁹*Departamento de Física, Universidad Nacional de Colombia, Bogota, Colombia
(associated with LPNHE, Sorbonne Université, Paris Diderot Sorbonne Paris Cité, CNRS/IN2P3, Paris, France)*

⁷⁰*Universität Bonn—Helmholtz-Institut für Strahlen und Kernphysik, Bonn, Germany
(associated with Physikalisches Institut, Ruprecht-Karls-Universität Heidelberg, Heidelberg, Germany)*

⁷¹*Eotvos Lorand University, Budapest, Hungary
(associated with European Organization for Nuclear Research (CERN), Geneva, Switzerland)*

⁷²*INFN Sezione di Perugia, Perugia, Italy
(associated with INFN Sezione di Ferrara, Ferrara, Italy)*

⁷³*Van Swinderen Institute, University of Groningen, Groningen, Netherlands
(associated with Nikhef National Institute for Subatomic Physics, Amsterdam, Netherlands)*

⁷⁴*Universiteit Maastricht, Maastricht, Netherlands
(associated with Nikhef National Institute for Subatomic Physics,
Amsterdam, Netherlands)*

⁷⁵*Tadeusz Kosciuszko Cracow University of Technology, Cracow, Poland
(associated with Henryk Niewodniczanski Institute of Nuclear Physics Polish Academy of Sciences,
Kraków, Poland)*

⁷⁶*DS4DS, La Salle, Universitat Ramon Llull, Barcelona, Spain
(associated with ICCUB, Universitat de Barcelona, Barcelona, Spain)*

⁷⁷*Department of Physics and Astronomy, Uppsala University, Uppsala, Sweden
(associated with School of Physics and Astronomy, University of Glasgow,
Glasgow, United Kingdom)*

⁷⁸*University of Michigan, Ann Arbor, Michigan, USA
(associated with Syracuse University, Syracuse, New York, USA)*

^aDeceased.

^bAlso at Università di Firenze, Firenze, Italy.

^cAlso at Scuola Normale Superiore, Pisa, Italy.

^dAlso at Università di Ferrara, Ferrara, Italy.

^eAlso at Università di Milano Bicocca, Milano, Italy.

^fAlso at Università di Bologna, Bologna, Italy.

^gAlso at Università di Genova, Genova, Italy.

^hAlso at Universidad Nacional Autónoma de Honduras, Tegucigalpa, Honduras.

ⁱAlso at Università di Bari, Bari, Italy.

^jAlso at Università di Cagliari, Cagliari, Italy.

^kAlso at Università di Perugia, Perugia, Italy.

^lAlso at Università di Roma Tor Vergata, Roma, Italy.

^mAlso at Universidade de Brasília, Brasília, Brazil.

ⁿAlso at Hangzhou Institute for Advanced Study, UCAS, Hangzhou, China.

^oAlso at Università di Siena, Siena, Italy.

^pAlso at Università degli Studi di Milano, Milano, Italy.

^qAlso at Central South U., Changsha, China.

^rAlso at Università di Padova, Padova, Italy.

^sAlso at Excellence Cluster ORIGINS, Munich, Germany.

^tAlso at Dipartimento MIFT, Università degli Studi di Messina and INFN Sezione di Catania, Italy, Messina and Catania, Italy.

^uAlso at Università di Pisa, Pisa, Italy.

^vAlso at Università della Basilicata, Potenza, Italy.

^wAlso at Universidad de Alcalá, Alcalá de Henares, Spain.

^xAlso at Università di Urbino, Urbino, Italy.